**Supplementary Information**

# The photo-assisted methane dry reforming over Ni-Co-$CeO_2$-$Al_2O_3$ catalyst with enhanced activity: synergistic effect of Ni and Co

Jiming Wang,[a] Min Ji*[a] and Min Wang*[a]

[a] School of Chemistry, Dalian University of Technology, Dalian 116024, PR China

E-mail: jimin@dlut.edu.cn, wangmin@dlut.edu.cn

## Kinetic studies

Determining the carbon gasification rate by using $CO_2$ oxidation of deposited carbon over spent catalysts was used as follows, which was based on a modified Wigner–Polanyi equation (often used to generate kinetic data for TPD process).[1] As only small amount of surface carbon was identified on spent catalysts, and most of which can be gasified by $CO_2$ via reverse Boudouard reaction (Eq. 1) to CO, by assuming that the reverse reaction and re-adsorption are negligible, the following gasification kinetic law (Eq. 2) applies to the $CO_2$ surface gasification process.[2] These conditions are satisfied under our $CO_2$-excessive $CO_2$-TPO conditions operating under the high flow rate of carrier gas (He, 30 ml $min^{-1}$), and first order reaction to surface carbon concentration was identified before.[1]

$$C^* + CO_2 = 2CO^* + * \quad (1)$$

$$r = -\frac{d\theta^*}{dt} = A\theta^* \exp[-\frac{E_a}{RT}] \times P_{CO_2}^n \quad (2)$$

Where A is the pre-exponential factor, θ* is the surface carbon coverage, $E_a$ is the activation energy and n is the reaction order with respect to $CO_2$ partial pressure. R and T are the universal gas constant and temperature, respectively. To determine the kinetic

parameters, A, n and $E_a$ need to be identified by regression. All samples were outgassed to 120 °C to remove surface contaminants during post-tests handlings under $N_2$ for 1 h, such as water. In the first series experiments, we used a tiny amount of spent catalysts (typically 10 mg) and a pure flow of $CO_2$, in order that the concentration variation of $CO_2$ can be deemed as constant. The samples placed at the bottom of the Ushaped quartz tube were investigated by heating the samples from 30 °C to 900 °C in $CO_2$ (100 vol.%) flow (30 ml $min^{-1}$) at heating rates of 4, 7, 10, 15 °C $min^{-1}$, respectively. The $CO_2$ consumption was monitored by a TCD. Under such circumstances, a pseudo zeroth kinetic order for $P_{CO_2}^n$ applies, and $E_a$ could therefore be measured by changing ramp of heating for $CO_2$-TPO,

$$r = -\frac{d\theta^*}{dt} = A\theta^* \exp[-\frac{E_a}{RT}] \times P_{CO_2}^n = AP_{CO_2}^n \theta^* \exp[-\frac{E_a}{RT}] \quad (3)$$

$AP_{CO_2}^n$ can be regarded as an invariable, for the exceedingly high partial pressure and small consumption.

During the TPO analysis, the temperature is increased linearly by:

$$T_t = T_0 + \beta t \quad (4)$$

Where = $\beta$ dT/dt and $T_0$ is the initial temperature. Thus:

$$-\frac{d\theta^*}{dT}\beta = AP_{CO_2}^n \theta^* exp[-\frac{E_a}{RT}] \quad (5)$$

If $T_M$ is the maximum temperature of a given TPO spectrum, then:

$$\frac{d}{dT}[\theta^* (\frac{AP_{CO_2}^n}{RT}) exp(\frac{E_a}{RT})] = 0 \quad (6)$$

$$2\ln T_M - \ln\beta = \frac{E_a}{RT_M} + \ln\left(\frac{E_a}{AP_{CO_2}^{n}R}\right) \quad (7)$$

$2\ln T_M - \ln\beta$ vs. $1/T_M$ curve can be used to deduce Ea from the slope.

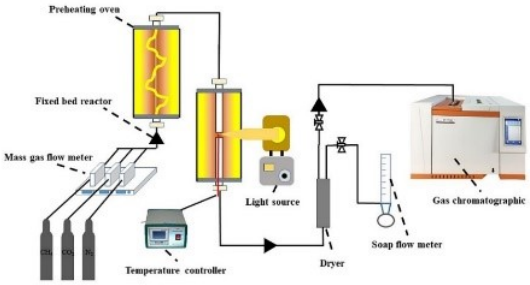


**Fig. S1** Diagram of experimental device.

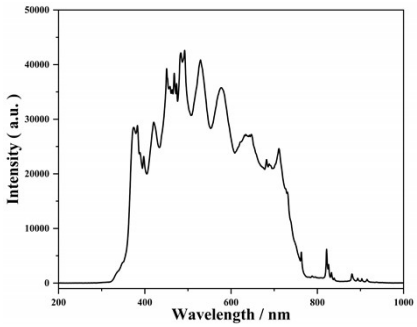


**Fig. S2** Spectrum of 300 W xenon light source intensity for PTC-DRM reaction.

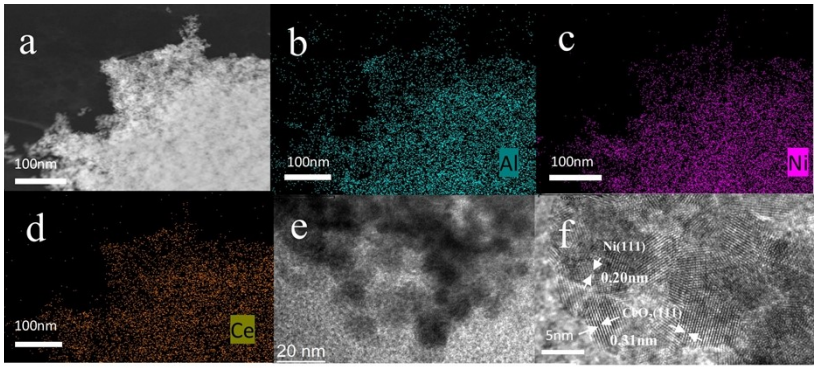


**Fig. S3** TEM images with element mapping (a-d), TEM (e), HRTEM (f) of the Ni-Ce-Al sample.

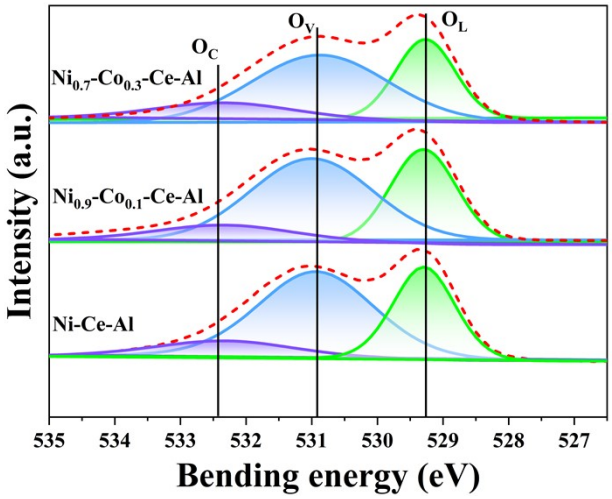


**Fig. S4** O 1 s XPS spectra of reduced Ni-Ce-Al, $Ni_{0.9}$-$Co_{0.1}$-Ce-Al and $Ni_{0.7}$-$Co_{0.3}$-Ce-Al.

**Table S1** XPS characterization results of the reduced catalysts

| Samples | Ni-Ce-Al | $Ni_{0.9}$-$Co_{0.1}$-Ce-Al | $Ni_{0.7}$-$Co_{0.3}$-Ce-Al |
|---|---|---|---|
| O 1s($O_V$/$O_C$) ratio | 3.29 | 3.18 | 2.97 |
| O 1s($O_V$/$O_L$) ratio | 1.29 | 1.22 | 1.18 |

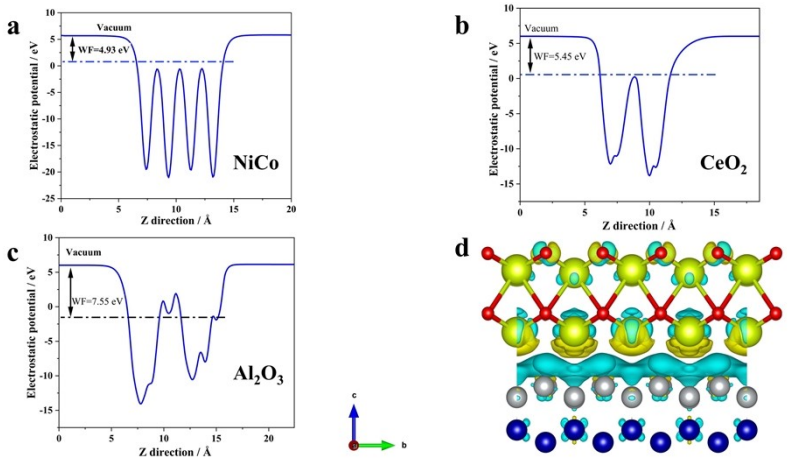


**Fig. S5** Electrostatic potentials of NiCo (a), $CeO_2$ (b), $Al_2O_3$ (c) and the side view (d).

**Table S2** Comparison of catalyst performance with data in the literature.

| Entry | Sample | Operating temperature (OA); Actual temperature of catalyst (AT) | Reactor type | Conditions | Production rates of CO and $H_2$ ($P_{CO}$ and $^{p}H_2$) | Ref |
|---|---|---|---|---|---|---|
| 1 | $10Ni/Al_2O_3$ | OT = 550 °C<br>AT = NR | Flow-type reactor | LA-251Xe lamp with a HA30 filter (UV-visible light of 300−800 nm, 1.07 W $cm^{-2}$); 50 mg sample; Total feed flow rate is 20.0 mL/min ($CH_4/CO_2$ = 1: 1); atmospheric pressure | $P_{CO} \approx 6.5$ μmol $min^{-1}$<br>$^{p}H_2 \approx 6$ μmol $min^{-1}$ | 3 |
| 2 | Pt/black $TiO_2$ | OT = 550 °C<br>AT = NR | Flow-type reactor | AM 1.5 G Newport solar simulator (100 mW/$cm^{-2}$); 15 mg sample; $CH_4/CO_2$ mixture gas ($CH_4/CO_2$= 1.0; GHSV = 40000 mL/$g_{cat}$/h) | $P_{CO}$ = 39 μmol $min^{-1}$<br>$^{p}H_2$ = 17 μmol $min^{-1}$ | 4 |
| 3 | Pt-Si-$CeO_2$ | OT = 600 °C<br>AT = 600 °C | Flow-type reactor | A custom-made solar simulator (250–800 nm, 1775 mW$cm^{-2}$); 10 mg sample; Total feed flow rate is 14 mL/min ($CH_4/CO_2$ = 1:1) | $P_{CO}$ = 24 μmol $min^{-1}$<br>$^{p}H_2$ = 15 μmol $min^{-1}$ | 5 |
| 4 | MgO/Pt/Zn-$CeO_2$ | OT = 600 °C<br>AT = 600 °C | Flow-type reactor | A concentrated solar simulator (1200 W); 5 mg sample; 10% $CH_4$ and 10% $CO_2$; Total feed flow rate is 14 mL/min ($CH_4/CO_2$ = 1:1); 1.01 × 105 Pa | $P_{CO}$ = 43 μmol $min^{-1}$<br>$^{p}H_2$ = 29 μmol $min^{-1}$ | 6 |
| 5 | $Ni_{0.9}$-$Co_{0.1}$-Ce-Al | OT = 650 °C<br>AT = 650 °C | Flow-type reactor | 300 W Xe-lamp; 60 mg sample; Total feed flow rate is 60.0 mL/min ($CH_4/CO_2$ = 1:1); atmospheric pressure | $P_{CO}$ = 27.7 μmol $min^{-1}$<br>$^{p}H_2$ = 23.6 μmol $min^{-1}$ | This work |

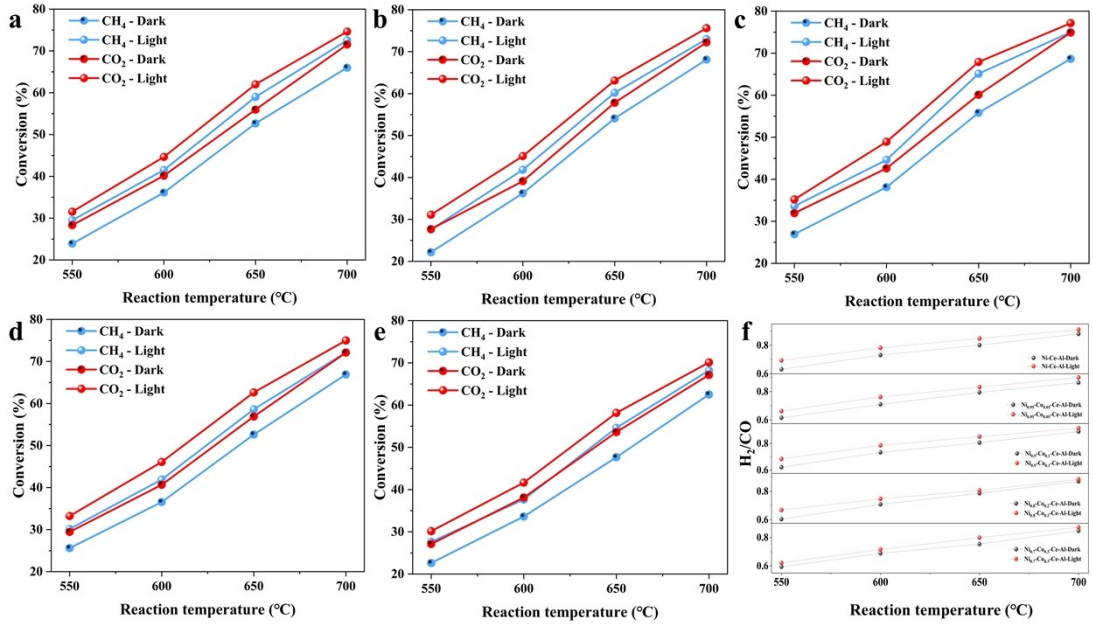


**Fig. S6** (a) Ni-Ce-Al, (b) $Ni_{0.95}$-$Co_{0.05}$-Ce-Al, (c) $Ni_{0.9}$-$Co_{0.1}$-Ce-Al, (d) $Ni_{0.8}$-$Co_{0.2}$-Ce-Al and (e) $Ni_{0.7}$-$Co_{0.3}$-Ce-Al catalysts for PTC-DRM reaction and (f) $H_2$/CO. (Reaction conditions:WHSV = 60000 mL·g$^{-1}$·h$^{-1}$, $CH_4$ / $CO_2$=1 / 1)

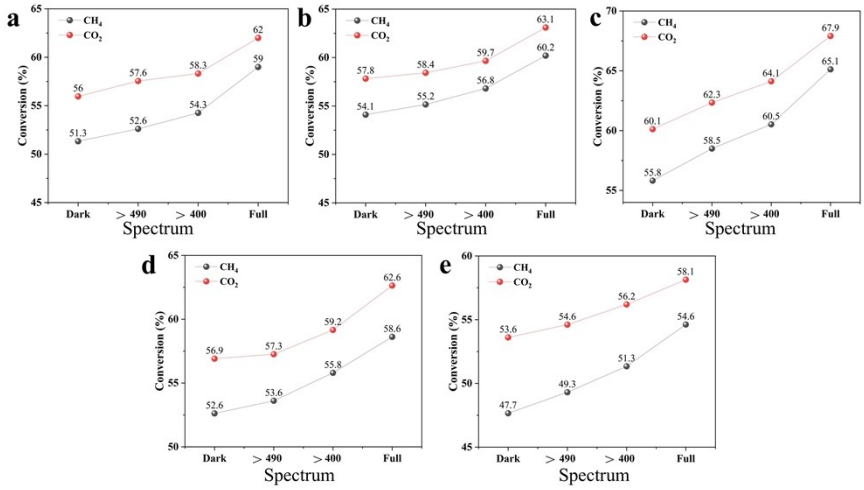


**Fig. S7** Effect of different wavelengths of light source at 650°C on the catalytic performance of (a) Ni-Ce-Al, (b) $Ni_{0.95}$-$Co_{0.05}$-Ce-Al, (c) $Ni_{0.9}$-$Co_{0.1}$-Ce-Al, (d) $Ni_{0.8}$-$Co_{0.2}$-Ce-Al and (e) $Ni_{0.7}$-$Co_{0.3}$-Ce-Al (Reaction conditions : WHSV=60000 mL·g$^{-1}$·h$^{-1}$, $CH_4$ / $CO_2$=1 / 1)

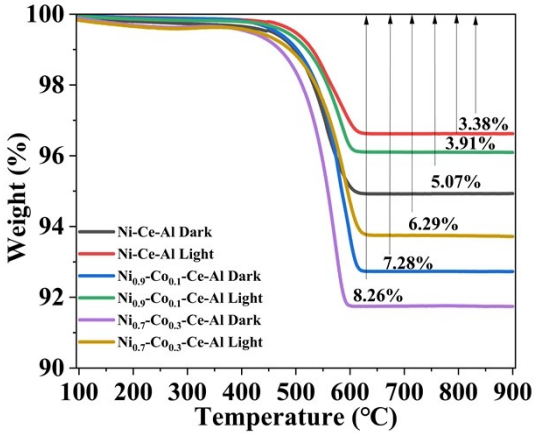


**Fig. S8** Thermogravimetric curves of Ni-Ce-Al, $Ni_{0.9}$-$Co_{0.1}$-Ce-Al and $Ni_{0.7}$-$Co_{0.3}$-Ce-Al catalysts after thermal catalytic and photothermal catalytic reactions.

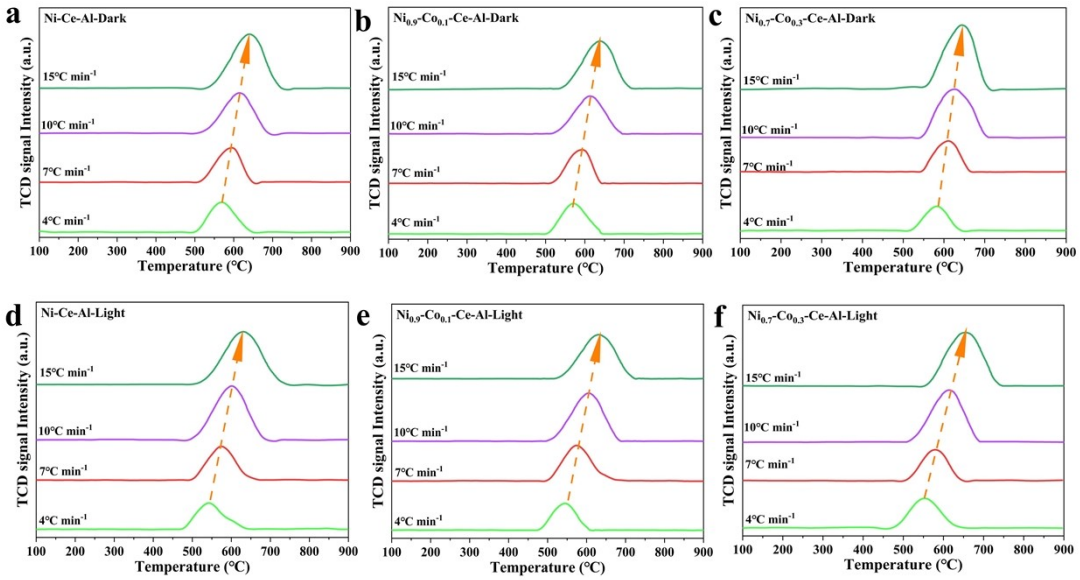


**Fig. S9** $CO_2$-TPO patterns for Ni-Ce-Al (a, d), $Ni_{0.9}$-$Co_{0.1}$-Ce-Al (b, e) and $Ni_{0.7}$-$Co_{0.3}$-Ce-Al (c, f) with manipulated heating rates of 4, 7, 10, 15 ℃ $min^{-1}$ from 100 ℃ to 900 ℃ under dark and light conditions respectively.

References:


1. H. Zhou, T. Zhang, Z. Sui, Y.-A. Zhu, C. Han, K. Zhu and X. Zhou, Appl. Catal. B-Environ. 2018, **233**, 143-159.
2. T. Osaki, Catal. Lett. 2015, **145**, 1931-1940.
3. H. Liu, H. Song, W. Zhou, X. Meng and J. Ye, Angew. Chemie Int. Ed. English, 2018, **57**, 16781-16784.
4. H. Liu, T.D. Dao, L. Liu, X. Meng, T. Nagao and J. Ye, Appl. Catal. B-Environ. 2017, **209**, 183-189.
5. F. Pan, X. Xiang, W. Deng, H. Zhao, X. Feng and Y. Li, ChemCatChem, 2018, **10**, 940-945.
6. F. Pan, X. Xiang, Z. Du, E. Sarnello, T. Li and Y. Li, Appl. Catal. B-Environ. 2020, **260**, 118189.